Applied Energy 278 (2020) 115686

Contents lists available at ScienceDirect

Applied Energy

journal homepage: www.elsevier.com/locate/apenergy

Assessing the mitigation of greenhouse gas emissions from a green infrastructure-based urban drainage system☆

Jiahong Liu [a,b,c,*], Jia Wang [a], Xiangyi Ding [a], Weiwei Shao [a], Chao Mei [a], Zejin Li [a], Kaibo Wang [a]

[a] State Key Laboratory of Simulation and Regulation of Hydrological Cycle in River Basin, China Institute of Water Resources and Hydropower Research, Beijing 100038, China
[b] School of Transportation and Civil Engineering & Architecture, Foshan University, Guangdong 52800, China
[c] Engineering and Technology Research Center for Water Resources and Hydroecology of the Ministry of Water Resources, Beijing 100038, China

HIGHLIGHTS

- City-scale method for greenhouse gas emissions mitigation of green infrastructure.
- Green infrastructure improves annual GHG mitigation levels by 45.9% on average.
- Annual greenhouse emission mitigation benefits are positive-skew distribution.
- Rainfall is positive non-linear correlated with greenhouse gas emissions mitigation.

GRAPHICAL ABSTRACT

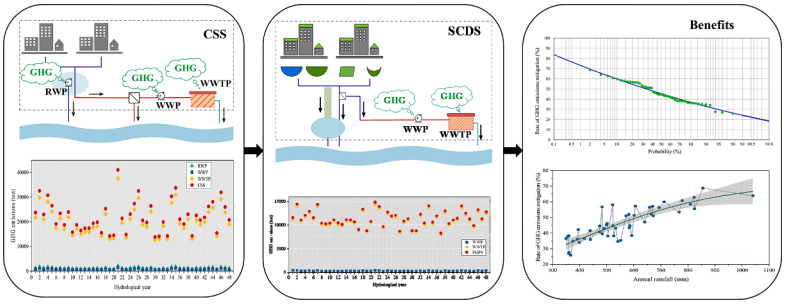

ARTICLE INFO

Keywords:
Green infrastructure
Rainwater management
Sponge city
Greenhouse gas mitigation effect
Urban drainage system

ABSTRACT

Green infrastructure (GI) is a low-carbon solution for urban rainwater management. Hydrological processes and the corresponding emissions of greenhouse gas (GHG) during rainfall events are optimized by GI when the latter is compared with a traditional urban drainage system. This study establishes an city-scale quantitative analysis, based on hydrological processes, with which to assess the contribution of GIs to low-carbon urban drainage systems and cities. The emission factor method is applied to measure GHG emissions. Attributable sources of emissions are wastewater treatment plants and wastewater and rainwater pumps. The amount and rate of change in GHG emissions were selected as indicators of the impacts of GI-based urban drainage systems and a case study was conducted in Dongying, China, based on 48 hydrological scenarios from 1970 to 2017. The amount of annual GHG emissions decreased by 3752.5 to 26238.9 tons of CO_2 equivalent at an average of 10677.3 tons/a. The rate of annual GHG emissions decreased by 25.9–68.7% with an average reduction of 45.9%. An S-shaped logistic curve fit the data, indicated that annual rainfall is non-linearly and positively correlated with both the amount and rate of annual GHG emissions mitigated. The probability of benefits to GHG emissions in the 48 hydrological scenarios is analyzed based on a Pearson type III distribution curve. These findings can provide information that

☆ The short version of the paper was presented at ICAE2019, Aug 12–15, Västerås, Sweden. This paper is a substantial extension of the short version of the conference paper.

* Corresponding author at: State Key Laboratory of Simulation and Regulation of Water Cycle in River Basin, China Institute of Water Resources and Hydropower Research, Beijing 100038, China.
E-mail address: liujh@iwhr.com (J. Liu).

https://doi.org/10.1016/j.apenergy.2020.115686
Received 25 February 2020; Received in revised form 24 June 2020; Accepted 25 July 2020
Available online 27 August 2020

local authorities can use to guide policies towards their goals of applying GIs to mitigate GHG emissions in the urban drainage system.

1. Introduction

Global warming has become a severe problem that cannot be ignored [1,2]. Climate change is accelerating and record greenhouse gas (GHG) concentrations are increasing global temperatures towards dangerous levels [3]. An increasing number of cities worldwide are currently aiming to develop low carbon models of development [4–6]. China is also playing an essential role in mitigating climate change [7,8]. At the World Climate Conference in Copenhagen, China promised to decrease carbon emissions by 60–65% per unit of GDP by 2030 from 2005 levels. The urbanization rate in China reached 60.60% at the end of 2019, indicating that this is still at a rapid development stage. China is thus under severe pressure to conserve energy and mitigate emissions in this field.

An urban drainage system usually consists of infrastructure for rainwater collection and drainage and wastewater collection, treatment, and discharge [9]. Rainwater and wastewater conveyance processes result in GHG emissions including indirect carbon dioxide emissions through the consumption of energy and direct emissions of carbon dioxide, nitrous oxide, and methane [10]. Urban runoff caused by the expansion of impervious surfaces is increasing against the backdrop of rapid urbanization [11]. Meanwhile, water consumption rates and the amount of wastewater generated are increasing with an increase in the urban population [12]. These trends warrant the continual expansion of the urban drainage system; consequently, energy consumption and GHG emissions increase. Predictably, an increasing number of cities are likely to adopt energy-saving or GHG emissions mitigation targets that will allow their urban drainage systems to cope with the increasingly critical conditions of climate change [13].

The construction of a traditional drainage system, particularly rainwater drainage systems, has many challenges. One of these is the rapid expansion of impervious surfaces, which increases the volume of runoff and peak flow and thereby leads to a severe risk of urban flooding. This leads to additional gray infrastructure, including pipe networks and large pumping stations, being constructed to prevent the flooding. This gray infrastructure aims to control urban flood only, further aggravating the damage to natural processes in the hydrological cycle [14]. Thus, despite the investment of money and energy, the risk of urban flooding is not fundamentally eliminated and the generation of GHG emissions increases during the construction and operation of the gray infrastructure [15]. Another challenge is that many cities around the world, especially old towns, have combined sewer systems (CSSs) in which rainwater runoff, domestic sewage, and industrial wastewater flow through the same pipe network, with rainwater runoff flowing into a wastewater treatment plant during rainfall events [16]. This increases the load at wastewater pumping stations and treatment plants and thereby increase GHG emissions unnecessarily. Finally, global warming means that the historical meteorological records, including the precipitation depth and rain intensity, have been inconsistent in recent years for areas that are urbanizing; this aggravates urban water issues and creates a vicious cycle [17].

China is now implementing the sponge city strategy nationwide to mitigate severe urban water challenges [18]. In this strategy, green infrastructure (GI) is adopted to create an urban hydrological cycle with benefits for all processes involved. These measures help promote the natural accumulation, infiltration, and purification of rainwater runoff. There are currently several concepts similar to the sponge city initiative, including low impact development, best management practices, sustainable urban drainage systems, and water sensitive urban design [19]. Implementation processes have focused on assessing the performance of GI in terms of flood control, improvements in runoff water quality, and cost-benefit analysis based on the aforementioned functions [20]; however, evidence of its impact on the mitigation of GHG emissions is still insufficient [21]. Despite this, governments and researchers are leaning towards using new concepts in integrated water management that consider the inclusion of new environmental quality indicators including GHG emissions [22].

The use of GI is a low-carbon rainwater management mode with great potential for mitigating climate change as it decreases the energy consumed in raw material production and transportation and facility construction, operation, and management when compared to gray infrastructure [23]. De Sousa et al. [24] used a life cycle assessment (LCA) to quantify the GHG emissions of GI and found that, over its life cycle, its GHG emissions were 75–95% lower than those of gray infrastructure options. Wang et al. [25] used an LCA approach to evaluate the trade-offs between improvements in water quality and the incremental climatic, resource, and economic costs of implementing GI versus gray infrastructure in a combined drainage system. Results showed that a combined sewer system of GI expansions provides more cost-effective improvement. Additionally, GI plays an important role in the sequestration of carbon in vegetation, indicating that it has a potential function as a carbon sink. Moore et al. [26] proposed a framework for predicting carbon footprints to allow the construction and maintenance of vegetated and non-vegetated rainwater infrastructure, as well as to measure the potential effect of carbon sequestration in vegetated green infrastructure. Bouchard et al. [27] examined the carbon sequestration function of a roadside vegetated filter strip and vegetated swale by determining the carbon density of soil samples from each. Kavehei et al. [28] evaluated the potential of different types of GI as carbon sinks and found that rain gardens provide the highest carbon sequestration potential and thus offsets its carbon footprint. Green roofs are a popular adaptation by which the mitigation of carbon emissions can be assessed because they can reduce building temperatures and thus reduce the energy consumed by air conditioning [29,30]. A review conducted by Berardi et al. [31] found that this energy-related effectiveness is the main reason for the widespread use of green roofs. Devkota et al. [32] evaluated the potential of generating energy savings using harvested rainwater as a non-potable water source for uses such as irrigation and toilet flushing. The aforementioned studies used the LCA method extensively; furthermore, they generally focused on the GHG emissions account of a single type of GI used LCA methodologies to compare GHG emissions from green and gray infrastructure alternatives. These assessments of GI carbon emissions were also mainly conducted on the site scale. The implementation of GI resulted in changes in the hydrological processes during rainfall events, which then reduced the amount of rainwater runoff flowing into traditional drainage systems, particularly combined sewer systems. This meant that the GHG emissions of the whole urban drainage system could be mitigated. However, there is still a lack of quantitative analyses related to GHG emissions. Describing and understanding GHG emissions at the city level is essential because cities are the focus of future climate change mitigation and adaptation measures [33]. Mannina et al. [34] proposed studying the carbon emissions reduction potential of cities, as a whole, via an integrated urban drainage system; however, the proposal lacks a quantitative analysis method. Therefore, given the lack of comprehensive and large-scale studies, the goal of this work was to quantitatively assess how and to what extent GIs could contribute towards the creation of low-carbon urban drainage systems and cities. Yet the complexity and size of urban drainage systems makes it difficult to quantify the total GHG emissions of an entire drainage system; therefore, this study addressed the theory of GHG emissions mitigation of GI-based urban drainage system. Furthermore, it proposed a quantitative method with which to

assess changes in GHG emissions by determining the mitigation benefit of GIs from traditional urban drainage systems in the hydrological cycle during rainfall events at a city-scale. This can comprehensively demonstrate the potential effects of GI on reducing GHG emissions.

2. Methodology

This study aimed to quantitatively assess the benefits of mitigating GHG emissions from the implementation of GI at a city scale during the hydrological processes. Fig. 1 shows the research framework. The overall methodology consisted of three unique steps. First, hydrological and remote sensing, as well as that on the status of and planning for CSS and sponge city drainage system (SCDS) in the research area were collected and were preprocessed as data sources for this study. Hydrological data were used to calculate the rainwater volume managed by attributable sources including rainwater pump (RWP), wastewater pump (WWP) and wastewater treatment plant (WWTP), and remote sensing data were used to determine land uses and calculate the comprehensive runoff coefficient of the study area. Second, the study boundary was determined and the emission factor method used to calculate the contribution of CH_4, N_2O, and CO_2 emissions from the CSS and SCDS in the hydrological process. Lastly, two indexes of the amount and rate of change in GHG emissions were selected to calculate the annual benefit of mitigating GHG emissions via the use of GI. A Pearson type III distribution curve was used to analyze the frequency of annual benefit of mitigating GHG emissions, and nonlinear logistic regression was used to analyze the relationship between the former and annual rainfall in different hydrological years.

2.1. Study area

The 323.8 km^2 area studied in this work is the built-up part of Dongying city, in the northeastern part of Shandong Province, China; it is in the delta of the Yellow River estuary. The rate of urbanization in Dongying is 69.04%. Fig. 2 shows the locations of and land uses in the study area. According to the 2017 and 2018 statistical yearbooks for Dongying, coal and petroleum account for more than 95% of the sources of primary energy consumed in the city, while natural gas accounts for less than 3%. Thermal power is the main source of electric power. Dongying has a temperate continental monsoon climate with an annual average rainfall of 550–600 mm. There are 10 WWTPs and 36 rainwater pumping stations in the study area, and the volume of sewage treated is approximately 385,000 m^3/d. In 2016, a Special Plan for Sponge City was initialized in central Dongying; the plan divided this area into 18 drainage sub-areas. A total annual runoff control rate of 75% can be achieved via the construction of GI in each of these areas that is designated a control unit. The datasets for the drainage systems were obtained mainly from planning documents and announcements from the municipal government of Dongying.

2.2. GHG emissions from different urban drainage systems

2.2.1. Combined sewer system (CSS)

Dongying city currently uses a CSS, which means that domestic wastewater and rainwater are collected and transported through the same pipe network. Recently, the CSS in part of the central Dongying was renovated to separate the drainage system from the combined system at the community scale. However, because the main interceptor pipelines are still combined, the different types of water will still eventually become mixed despite this change. The boundary of study and the attributable sources of emissions of GHG emissions of CSS in the hydrological process are shown in Fig. 3. During a rainfall event, rainwater runoff flows into the main interceptor pipeline through rainwater pipes. When the volume of runoff exceeds the drainage capacity of

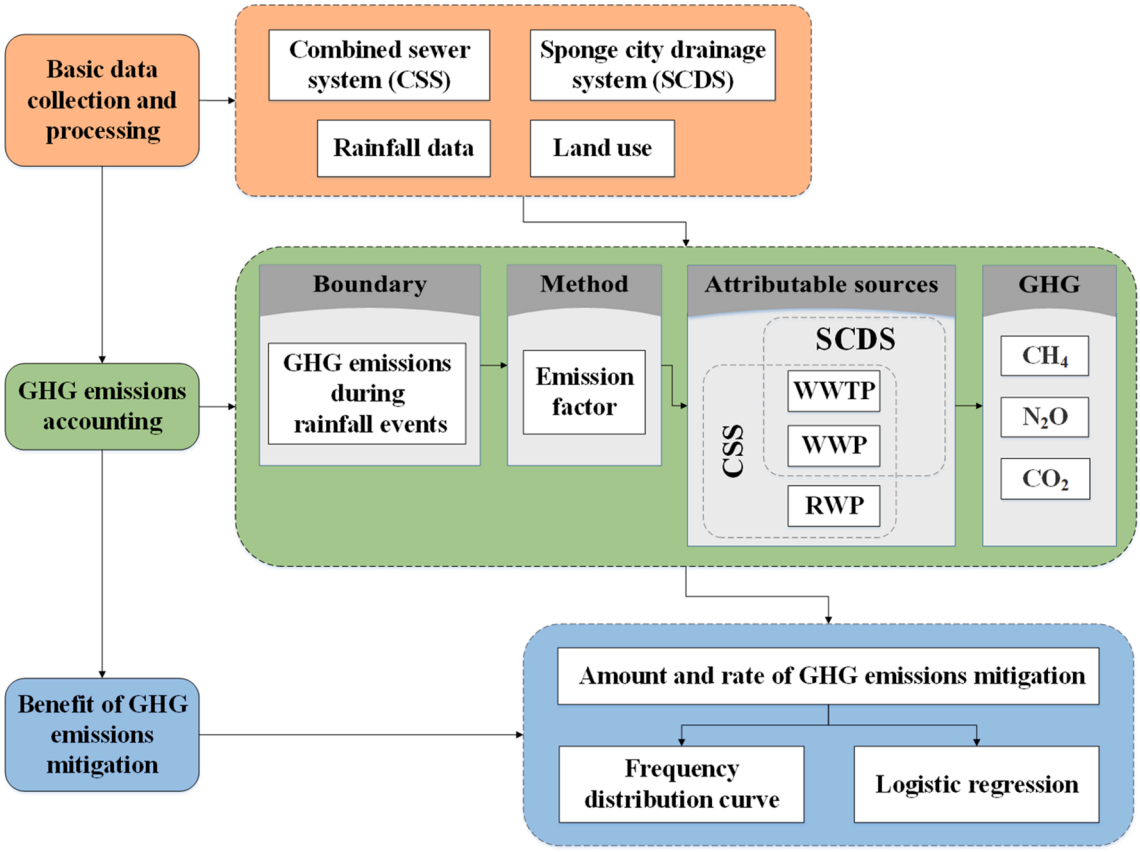

Fig. 1. Overall research framework.

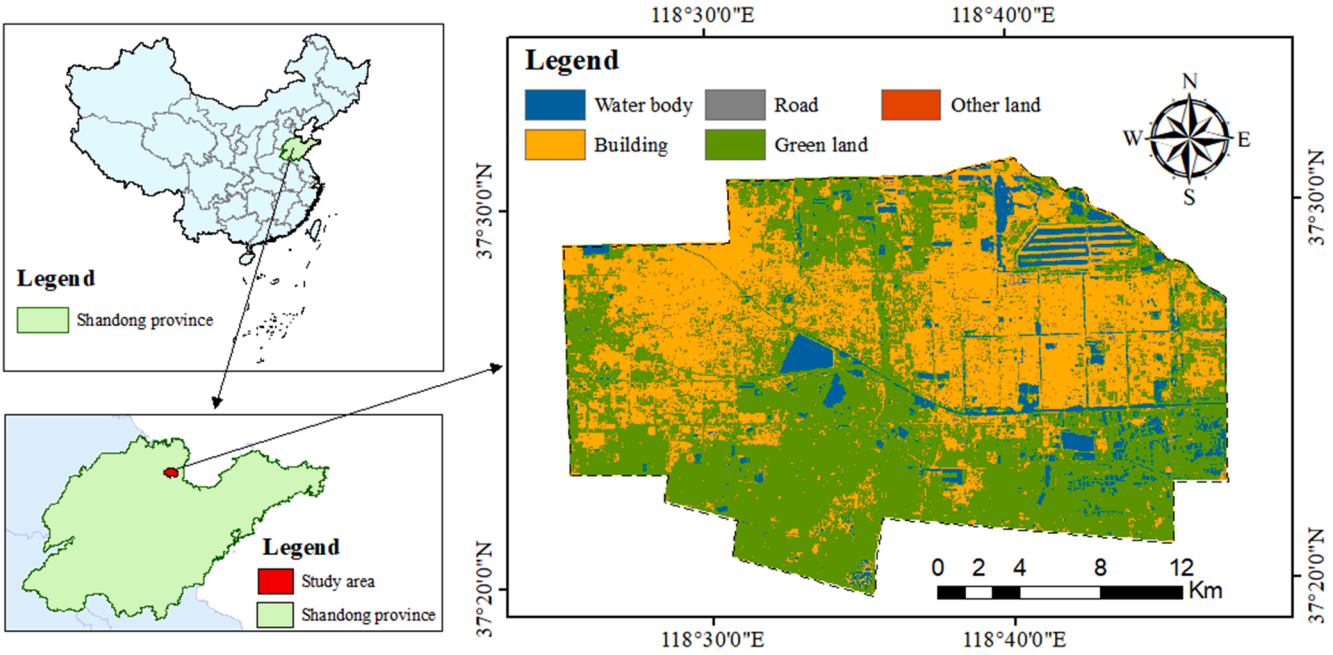

Fig. 2. Location of and distribution of land use in the study area.

rainwater pipes, the overflow causes urban flooding in low-lying areas. This floodwater is then removed into nearby water bodies using RWPs that consume electricity. Simultaneously, rainwater and wastewater are mixed in the main interceptor pipeline and discharged through the WWPs to WWTPs, which also consumes electricity as well as generating GHGs. During periods of heavy rainfall, the volume of mixed sewage in the CSS can exceed the capacity of the sewer system or WWTPs, and the occasional overflow is discharged directly into nearby water bodies. During rainfall events, the CSS carrying mixed rainwater runoff generates additional GHG emissions.

2.2.2. Sponge city drainage system (SCDS)

Dongying is constructing an SCDS, in which GI is used to restore natural hydrological cycle processes [35] to resolve the disadvantages of a traditional CSS. The SCDS is a comprehensive method by which to alleviate urban flooding and it effectively manage combined sewer overflows [36]. Moreover, GI has proved to be low-cost and low-carbon throughout its entire life cycle [37]. The extent of this study and the

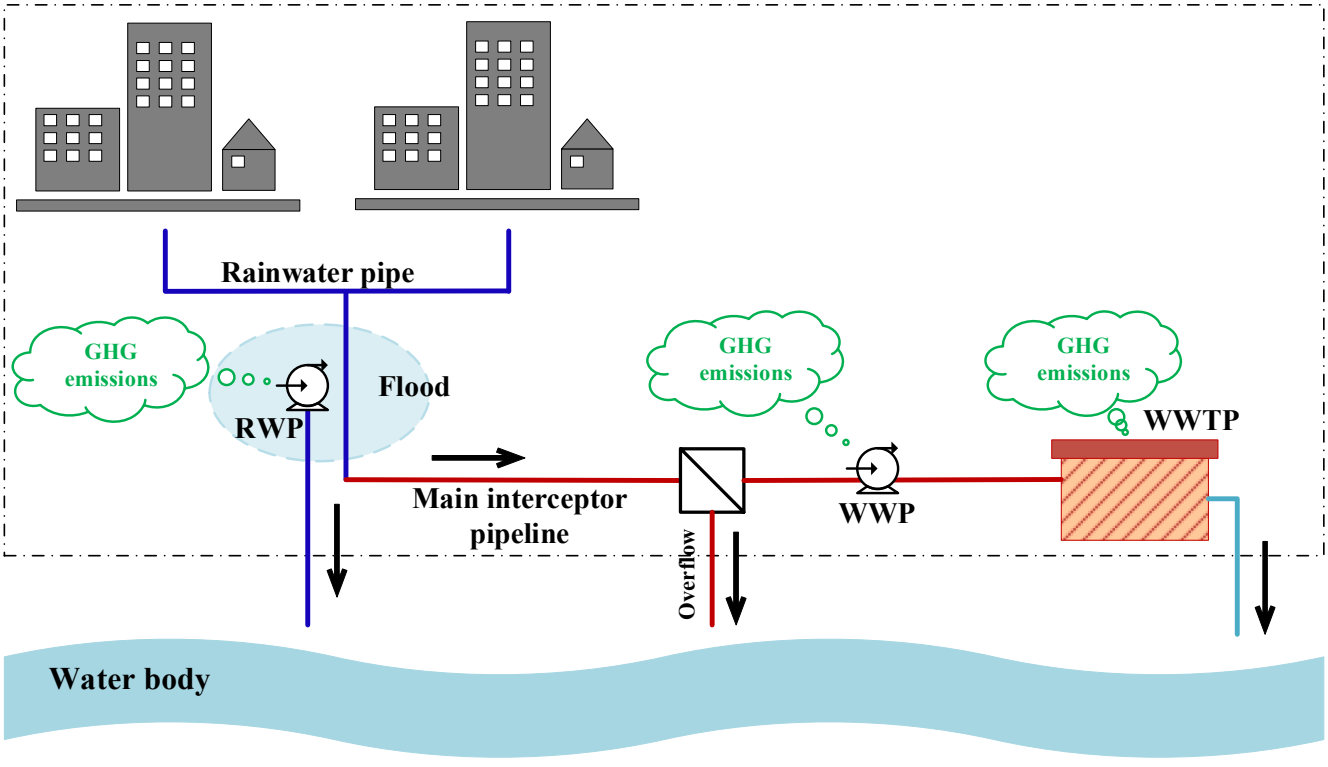

Fig. 3. Study boundary and the account of GHG emissions of CSS.

attributable sources of GHG emissions in the hydrological process of the SCDS are shown in Fig. 4. In the SCDS, rainwater runoff is first stored and purified using small-scale and decentralized GIs–including green roofs, bioretention basins, permeable pavements, rain gardens, and vegetated swales–at its sources; this reduces its volume and pollutant load. The overflow runoff that exceeds the processing capacity of these GIs is drained directly through rainwater pipes before being discharged into the nearest water body. If stormwater runoff exceeds the drainage capacity of the rainwater pipes, it is directed into a large waterway, stormwater pond/wetland via a gravity flow before it causes any urban flooding and then is discharged into the nearest water body. The RWPs in the traditional CSS have been replaced by this large-scale GI, thus reducing the energy consumption and GHG emissions corresponding to the former. Simultaneously, a small amount of the initial rainwater runoff, containing serious pollutants, is transported by WWP to a WWTP via split-flow, thereby consuming electricity and generating GHGs. The SCDS is therefore effective at reducing the amount of rainwater runoff flowing into WWTPs and WWPs, compared with the CSS, and is more effective at managing rainwater runoff; it thus reduces the energy consumption and corresponding GHG emissions of WWTPs and WWPs.

2.2.3. Mitigating GHG emissions via GI: The theory

The benefits of mitigating GHG emissions via GI come from adjustments to hydrological functions in a manner that differs from those caused by gray infrastructure. Fig. 5 shows the theory of how GI can mitigate GHG emissions, for example by effectively reducing rainwater runoff volumes and flattening runoff during hydrological processes through "infiltration, interception, storage and reuse" functions. In terms of the attributable sources of GHG emissions, implementing GI effectively reduces the volume of water entering RWPs; in a CSS, it performs the same function for WWPs and WWTPs and thus mitigates the corresponding GHG emissions. Accounting is done by calculating the benefit to daily GHG emissions mitigation of using daily rainfall and daily runoff reduction by the GI and then obtaining the annual benefit from the accumulative effect of this daily performance.

2.3. GHG emissions accounting

Both direct and indirect GHG emissions from the hydrological processes of urban drainage systems are generated mainly during different operations to deal with rainwater runoff. WWTPs are known to be one of the many contributors to GHG emissions. The treatments that occur at WWTPs result in direct emissions of GHGs including CO_2, CH_4, and N_2O, produced during physico-chemical or biological processes [38,39]. While CO_2 is also produced indirectly, through energy consumed by WWTPs, the carbon footprint of RWPs and WWPs come from indirect GHG emissions generated from their use of electricity. Furthermore, the dominant form of power generation is still based on fossil fuels, particularly coal, in China [40]. The anaerobic–anoxic–aerobic (AAO) process is applied widely in WWTPs in Dongying. The emission factor method can be applied to account for GHG emissions from this process, as in a study by Yan et al. [41], who analyzed AAO processes used in China and obtained the GHG emission factor thereof; this value was used as the data source for direct GHG emissions factors in this study. The ambient temperature during different seasons also affects the AAO process in WWTPs and will thereby have a certain impact on the determination of direct GHG emissions factors thereof [42]. As precipitation occurs in Dongying mainly during and around summer (rainfall from May to September accounts for more than 80% of the annual total), seasonal changes were not taken into account in this study. Emission factors for the 2017 regional grid baseline in North China were used as the source for indirect CO_2 emissions [43]. Table 1 shows the emission factors for

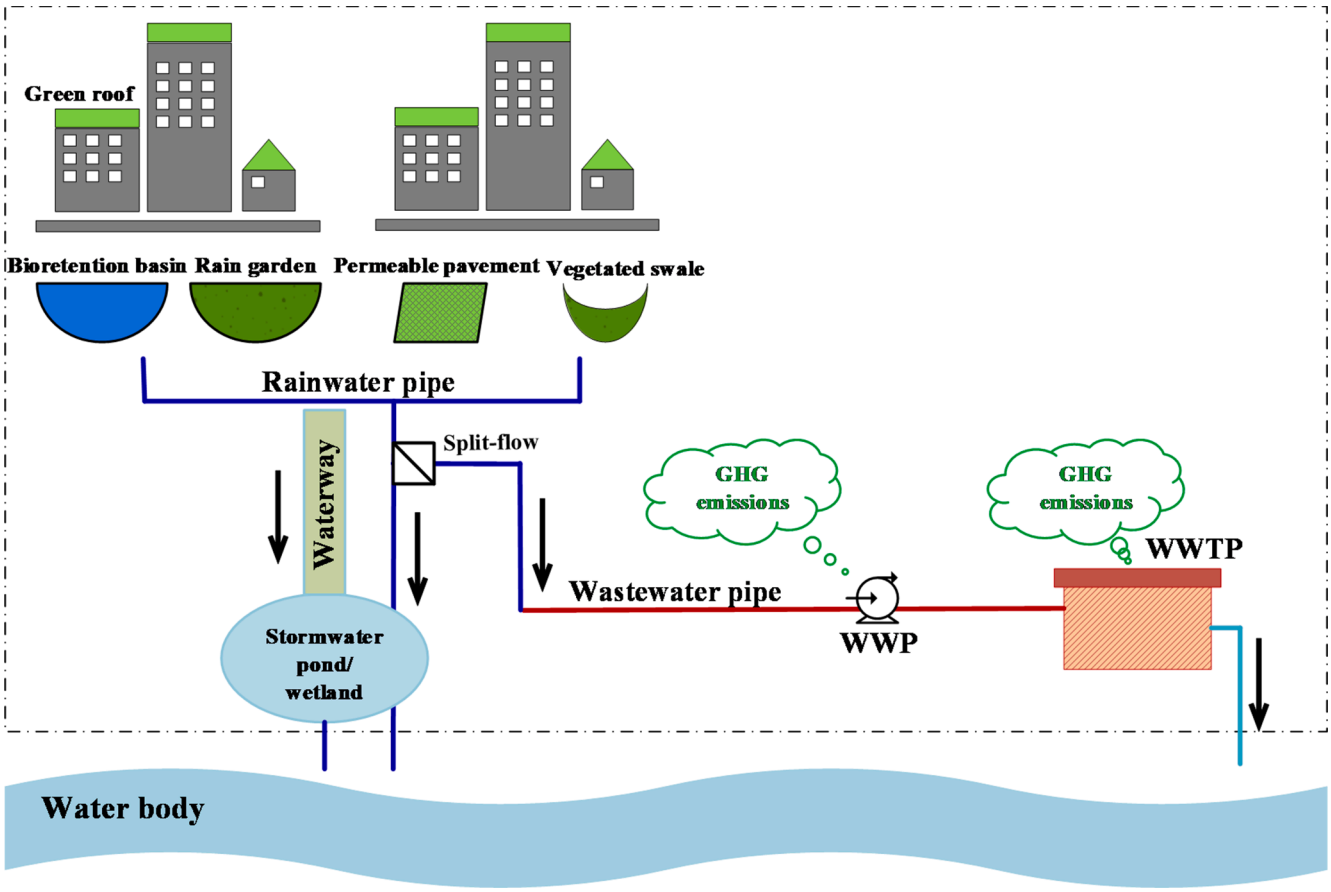

Fig. 4. Study boundary and the account of GHG emissions of SCDS.

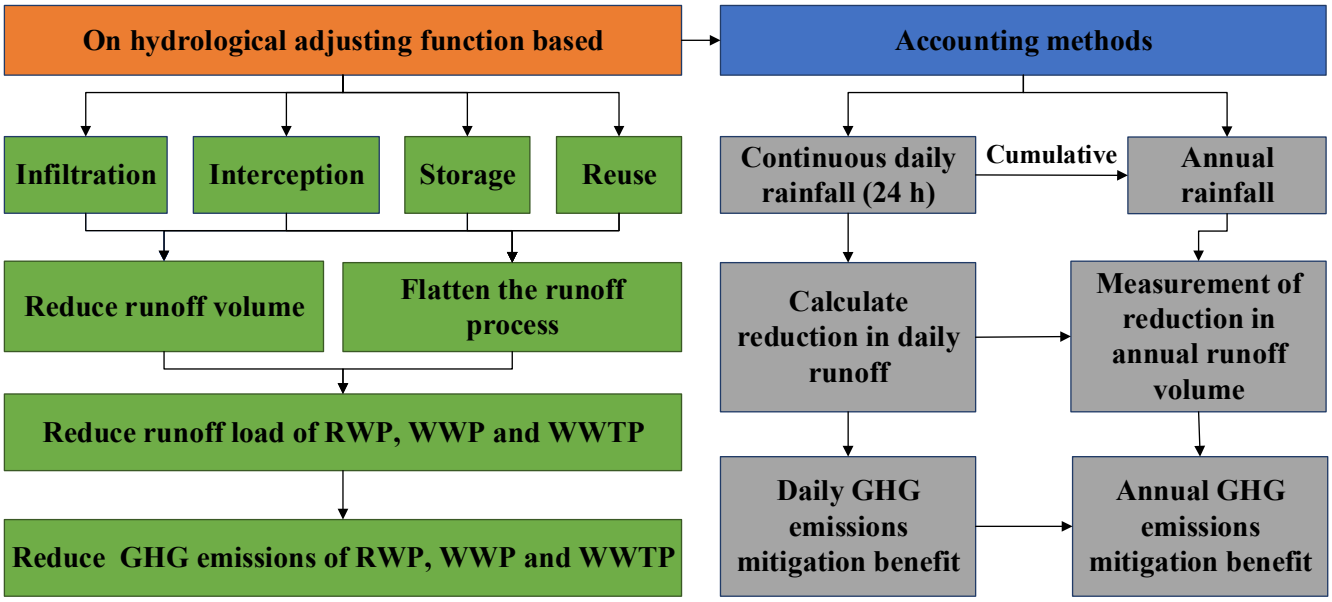

Fig. 5. Mitigating GHG emissions via GI: the theory.

CO_2, CH_4, and N_2O from WWTPs, RWPs, and WWPs.

2.3.1. Attributable sources of GHG emissions

(i) GHG emissions from WWPs

The main source of energy for WWPs is electricity. The power consumed in the operation of the WWPs to deliver rainwater runoff was calculated using Eq. (1) [44]:

$$EC_{WWP} = \frac{\rho g h Q_{WWP}}{3.6 \times 10^6 \times \eta} \quad (1)$$

where EC_{WWP} is the power consumed in the operation of WWPs (KWh); ρ is the density of water (kg/m^3); g is the gravitational acceleration (m/s^2); h is the average head of WWPs (m); Q_{WWP} is the amount of rainwater runoff discharge through WWPs (m^3); and η is the efficiency of the WWP engine.

In a CSS, some rainwater will be intercepted with wastewater and delivered to WWTPs through WWPs during rainfall events. The amount of water intercepted was calculated using Eq. (2):

$$Q_{WWP-CSS} = 10\alpha P_a F \varphi \quad (2)$$

where $Q_{WWP\text{-}CSS}$ is the volume of rainwater runoff intercepted by WWPs in a CSS (m^3); P_a is the annual rainfall (mm); F is the service area of the WWPs (ha); φ is the comprehensive runoff coefficient; and α is the interception coefficient, which is the proportion of the interception amount to the annual runoff.

In a SCDS, a small volume of initial rainwater runoff that includes serious runoff pollution will be transported to WWTPs by WWPs via split-flow systems that consume electricity and generate GHGs. This split-flow volume was calculated, according to the daily rainfall data from local hydrological stations, using Eq. (3):

$$Q_{WWP-SCDS} = q_s \times D + \sum q_i \quad (3)$$

where $Q_{WWP\text{-}SCDS}$ is the amount of rainwater runoff intercepted by WWPs in a SCDS (m^3); q_s is the design standard for initial rainwater interception; q_i is the daily rainfall which less than the value of q_s; i is the number of days when total daily rainfall is less than q_s; and D is the number of days when daily rainfall is more than q_s throughout the year.

GHG emissions from the electricity consumed by WWPs were calculated using Eq. (4):

$$E_{CO_2-WWP} = EC_{WWP} \times EF_{WWP} \quad (4)$$

where $E_{CO2\text{-}WWP}$ represents GHG emissions from the consumption of electricity by WWPs (kg); EC_{WWP} is the consumption of power by WWPs (KWh); and EF_{WWP} is the emission factor for electricity consumption by WWPs.

(ii) GHG emissions from WWTPs

The volume of rainwater runoff flow into WWTPs is the same as that for WWPs and was calculated using Eq. (5):

$$\begin{cases} Q_{WWTP-CSS} = Q_{WWP-CSS} \\ Q_{WWTP-SCDS} = Q_{WWP-SCDS} \end{cases} \quad (5)$$

where $Q_{WWTP\text{-}CSS}$ is the amount of rainwater runoff intercepted by WWTPs in a CSS (m^3); $Q_{WWP\text{-}CSS}$ is the volume of rainwater runoff intercepted by WWPs in a CSS (m^3); $Q_{WWTP\text{-}SCDS}$ is the volume of

Table 1
Emission factors of CO2, CH4, and N2O from WWTPs, RWPs and WWPs [41,43].

		Emission factor		
		WWTPs	WWPs	RWPs
Direct GHG emissions	CH4 (kg CH_4/m^3 sewage)	0.0004.	–	–
	N_2O (kg N_2O/m^3 sewage)	0.00006.	–	–
	CO_2 (kg CO_2/m^3 sewage)	0.1557.	–	–
Indirect GHG emissions	CO_2 (kg CO_2/kWh)	0.968.	0.968	0.968

rainwater runoff intercepted by WWTPs in a SCDS (m^3); and $Q_{WWP\text{-}SCDS}$ is the volume of rainwater runoff intercepted by WWPs in a SCDS (m^3).

Direct GHG emissions of CH_4, N_2O and CO_2 from WWTPs were calculated using Eq. (6):

$$\begin{cases} DE_{CH_4-WWTP} = Q_{WWTP} \times EF_{CH_4} \\ DE_{N_2O-WWTP} = Q_{WWTP} \times EF_{N_2O} \\ DE_{CO_2-WWTP} = Q_{WWTP} \times EF_{CO_2} \end{cases} \quad (6)$$

where DE_{CH4}, DE_{N2O}, and DE_{CO2} are the direct CH_4, N_2O, and CO_2 emissions from WWTPs when rainwater runoff is being treated (kg); Q_{WWTP} is the volume of rainwater runoff entering WWTPs; and EF_{CH4}, EF_{N2O}, and EF_{CO2} are the emissions factors for CH_4, N_2O, and CO_2, respectively.

The power consumed in the operation of WWTPs treating rainwater runoff was calculated using Eq. (7):

$$EC_{WWTP} = Q_{WWTP} \times EC_{average} \quad (7)$$

where EC_{WWTP} is the power consumed in the operation of WWTPs (KWh); Q_{WWTP} is the volume of rainwater runoff entering the WWTPs (m^3); and $EC_{average}$ is the average power consumed by WWTPs in Dongying (kWh/m^3), which is 0.29 kWh/m^3 [45].

Indirect GHG emissions of CO_2 from electricity consumed by WWTPs were calculated using Eq. (8):

$$InDE_{CO_2-WWTP} = EC_{WWTP} \times EF_{WWTP} \quad (8)$$

where $InDE_{CO2\text{-}WWTP}$ represents the indirect CO_2 emission of WWTPs (kg); EC_{WWTP} is the power consumed in the operation of WWTPs (KWh); and EF_{WWTP} is the emission factor for electricity consumed by WWTPs.

To facilitate data analysis, the N_2O and CH_4 emissions were converted into CO_2 equivalents. According to the Intergovernmental Panel on Climate Change [46], CH_4 and N_2O each have a strong global warming potential, at 25 and 298 times the global warming potential of CO_2, respectively, over 100 years. The total CO_2 equivalent emissions from WWTPs were thus calculated using Eq. (9):

$$EE_{CO_2-WWTP} = InDE_{CO_2-WWTP} + DE_{CO_2-WWTP} + T_{CH_4} \times DE_{CH_4-WWTP} + T_{N_2O} \times DE_{N_2O-WWTP} \quad (9)$$

where $EE_{CO2\text{-}WWTP}$ represent the total CO_2 equivalent emissions from WWTPs (kg); $InDE_{CO2\text{-}WWTP}$ represents the indirect CO_2 emissions from WWTP (kg); $DE_{CO2\text{-}WWTP}$, $DE_{CH4\text{-}WWTP}$, $DE_{N2O\text{-}WWTP}$ are, respectively, the direct emissions of CO_2, CH_4, and N_2O from WWTPs for treating rainwater runoff (kg); and T_{CH4} and T_{N2O} are the CO_2 equivalent emissions with global warming potential.

(iii) GHG emissions from rainwater pumps

The volume of rainwater runoff discharged annually by RWPs in a CSS was obtained using Eq. (10) [47]:

$$Q_{RWP-CSS} = 10 P_a F \varphi - Q_{WWP-CSS} \quad (10)$$

where $Q_{RWP\text{-}CSS}$ is the volume of rainwater runoff discharged by RWPs (m^3); P_a is the annual rainfall level (mm); F is the service area covered by RWPs (ha); φ is the coefficient of comprehensive runoff; and $Q_{WWP\text{-}CSS}$ is the volume of rainwater runoff flow into WWPs (m^3).

The power consumed by the operation of the RWPs to transport rainwater runoff was calculated using Eq. (11):

$$EC_{RWP} = \frac{\rho g h Q_{RWP}}{3.6 \times 10^6 \times \eta} \quad (11)$$

where EC_{RWP} is the power consumed in the operation of RWPs (KWh); ρ is the density of water passing through the RWPs (kg/m^3); g is the gravitational acceleration (m/s^2); h is the average head of the RWPs (m); Q_{RWP} is the volume of rainwater runoff discharged through the RWPs (m^3); and η is the efficiency of the RWP engine.

The main GHG emissions from electricity consumed by the RWPs were calculated using Eq. (12):

$$E_{CO_2-RWP} = EC_{RWP} \times EF_{RWP} \quad (12)$$

where $E_{CO2\text{-}RWP}$ represents the GHG emissions from the electricity consumed by the RWPs (kg); EC_{RWP} is the power consumed in the operation of the RWPs (KWh); and EF_{RWP} is the emission factor for electricity consumed by the RWP.

2.3.2. Urban drainage system

(i) CSS

The total GHG emissions from a CSS were calculated using Eq. (13):

$$E_{CO_2-CSS} = E_{CO_2-RWP-CSS} + EE_{CO_2-WWTP-CSS} + E_{CO_2-WWP-CSS} \quad (13)$$

where $E_{CO2\text{-}CSS}$ represents the total direct and indirect GHG emissions from a CSS (kg); $E_{CO2\text{-}RWP\text{-}CSS}$ stands for the GHG emissions from the electricity consumed by RWPs (kg); $EE_{CO2\text{-}WWTP\text{-}CSS}$ represents the total CO_2 equivalent emissions from WWTPs (kg); and $E_{CO2\text{-}WWP\text{-}CSS}$ stands for the GHG emissions from electricity consumed by WWPs (kg).

(ii) SCDS

The total GHG emissions from a SCDS were calculated using Eq. (14):

$$E_{CO_2-SCDS} = EE_{CO_2-WWTP-SCDS} + E_{CO_2-WWP-SCDS} \quad (14)$$

where $E_{CO2\text{-}SCDS}$ represents the total direct and indirect GHG emissions from a SCDS (kg); $EE_{CO2\text{-}WWTP\text{-}SCDS}$ represents the total CO_2 equivalent emissions from WWTPs (kg); and $E_{CO2\text{-}WWP\text{-}SCDS}$ stands for the GHG emissions from electricity consumed by WWPs (kg).

2.4. Benefits

2.4.1. Amount and rate of change of GHG emissions

The amount and rate of change of GHG emissions are two indicators usually used to analyze the benefit and potential of emissions mitigation [48,49]. Therefore, these two factors –as calculated from attributable sources–were selected as indicators with which to represent the benefit of GHG emissions mitigation using GIs before and after the implementation of the sponge city plan. These factors, as applicable to a change from a CSS to a SCDS, were calculated using Eq. (15):

$$\begin{cases} B_{amountofchange} = E_{CO_2-CSS} - E_{CO_2-SCDS} \\ R_{rateofchange} = B_{amountofchange} / E_{CO_2-CSS} \end{cases} \quad (15)$$

where $B_{amount\ of\ change}$ is the change in GHG emissions due to mitigation via the implementation of GI (kg); $R_{rate\ of\ change}$ is the rate of change in GHG emissions due to mitigation by GI; $E_{CO2\text{-}CSS}$ represents the total direct and indirect GHG emissions from a CSS (kg); and $E_{CO2\text{-}SCDS}$ stands for the total direct and indirect GHG emissions from a SCDS (kg).

2.4.2. Graphical analysis

An S-shaped logistic curve was used to analyze the variation in the amount and rate of change in GHG emissions based on annual rainfall. The logistic function is expressed as in Eq. (16):

$$y = a/(1 + b^* exp(-k^* x)) \quad (16)$$

where a, b, and k are parameters that shape and scale the function.

2.4.3. Analysis of distribution

The Pearson Type III distribution curve was adopted as best fitting the pattern of the benefits from GHG emissions mitigation. The

probability density function of this distribution is expressed as in Eq. (17):

$$f(x) = \frac{\beta^{\alpha}}{\Gamma(\alpha)}(x - a_0)^{\alpha-1} e^{-\beta(x-a_0)} \quad (17)$$

where $\alpha = 4/C_S^2$; $\beta = 2/\overline{x}C_V C_S$; $a_0 = \overline{x}(1 - 2C_V/C_S)$; C_V is the coefficient of variation; and C_S is the coefficient of skewness.

2.5. Assumptions

To make the case study as generic as possible, the following four assumptions were made:

(1) In a CSS, the volume of rainwater runoff entering WWPs and WWTPs is affected by rainfall, the size of WWPs, and the scale of WWTPs. However, this study did not consider these effects; a simplified method assuming that the amount of water entering the WWPs and WWTPs during rainfall events was subject to a uniform interception coefficient was utilized instead.
(2) In a CSS, the volume of rainwater runoff delivered by RWPs depends on the volume of water drained during urban flooding in a heavy storm. As the volume of floodwater generated is difficult to obtain at a city scale, this study adopted an estimation method based on Chen et al. [47]; the latter assumes that all rainwater runoff that does not enter WWPs is discharged by the RWPs.
(3) For a SCDS, this study proposed a simplified calculation method with which to determine the volume of initial rainwater runoff entering WWPs and WWTPs. It is assumed that all runoff from events in which rainfall is $\leq$3 mm enter WWPs and WWTPs while in those from events in which rainfall is >3 mm, 3 mm of rainwater enters WWPs and WWTPs based on the daily rainfall data.
(4) The GHG emissions from rainwater runoff are assumed to be subject to the average GHG emission level thereof without considering the differences in the characteristics of rainwater and wastewater quality. This is a simplification, as the efficiency of treatment and subsequent concentration of pollutants in effluent depends on its concentration in the influent. However, GHG emissions have only been considered in terms of the influence of different treatment processes in WWTPs.

The sources of data and value assumptions for different variables in this study are listed in Table 2.

3. Results and discussion

3.1. Analysis of rainfall characteristics

Fig. 6 shows daily rainfall statistics for the study area from 1970 to 2017. The amount of rainfall over the 48 hydrological scenarios used in this study ranges from 349.7 to 1039.7 mm. Rainfall levels are mainly low and medium, and the number of days on which daily rainfall is less than 25 mm accounts for 90.9% of the total days on which there is rainfall. The total rainfall from May to September accounts for 82.4% of the total rainfall; the extreme rainstorms that cause both drought and floods also occur mostly during this period. Fig. 7 shows the rainfall days and the corresponding total daily rainfall, both less and greater than 3 mm over 48 hydrological years, used to calculated Eq. (3).

3.2. GHG emissions from a CSS

The GHG emissions from a CSS during rainfall events were analyzed for each of the attributable sources examined in this study: WWPs, WWTPs, and RWPs. The different hydrological years are numbered 1–48 in sequence. In the 48 hydrological scenarios considered from 1970 to 2017, the annual CO_2 equivalent emissions from WWPs, WWTPs, and RWPs range from 477.1 to 1419.4 tons with an average of 763.6 tons, 12617.8 to 37514.1 tons with an average of 20181.1 tons, and 716.1 to 2129.1 tons with an average of 1145.4 tons, respectively. This is shown in Fig. 8.

3.3. GHG emissions from a SCDS

The GHG emissions from a SCDS during rainfall events were analyzed for different attributable sources including WWPs and WWTPs. In the 48 hydrological scenarios considered from 1970 to 2017, the annual CO_2 equivalent emissions of WWPs and WWTPs range from 228.1 to 421.8 tons with an average of 317.1 tons and 8037.2 to 14414.6 tons with an average of 11095.7 tons, respectively, as shown in Fig. 9.

3.4. Curve fitting for graphical analysis

Figs. 10 and 11 show the logistic curves that fit amount and rate of GHG emissions mitigated, respectively, using annual rainfall data from 48 hydrological scenarios. The rainfall amount generated across the 48 hydrological scenarios ranges from 349.7 to 1039.7 mm. These results indicate that amount and rate of GHG emissions mitigation increase with increases in annual rainfall. It is clear that increased rainfall will lead to an increased load on a CSS, thereby increasing GHG emissions also. In a SCDS, the vast majority of rainfall volume is managed by the GI that regulates hydrological processes, when only the initial rainfall is discharged into WWPs and WWTPs in the form of a split-flow. The GHG emissions from a SCDS does not depend on an increase of rainfall. Moreover, one benefit of the mitigation of GHG emissions from the GI is the impact on the cumulative effect of daily rainfall. A positive correlation is reasonable.

The parameter estimates and statistics derived from the fit of the logistic function using annual rainfall and the amount and rate of GHG emissions mitigated are shown in Table 3. The adjusted R^2 of the curve in Fig. 10 is 0.95, indicating a significant correlation between annual

Table 2
Sources of data and value assumptions for different variables in this study.

	Hydrological data	Daily rainfall measured at a local hydrological station from 1970 to 2017		
Data source	Remote sensing images	Google Earth		
	Land uses and runoff coefficients	Land use	Ratio	Runoff coefficient
		Water body	7.5%	1
		Building	39.6%	0.95
		Road	1.9%	0.95
		Green land	51%	0.25
		Comprehensive runoff coefficient: 0.6		
Value assumptions for different variables	Efficiency of engines at WWPs	0.75		
	Average head of WWPs (m)	5		
	Efficiency of engines at RWPs	0.75		
	Average head of RWPs (m)	5		
	Split-flow in a SCDS (mm)	3		

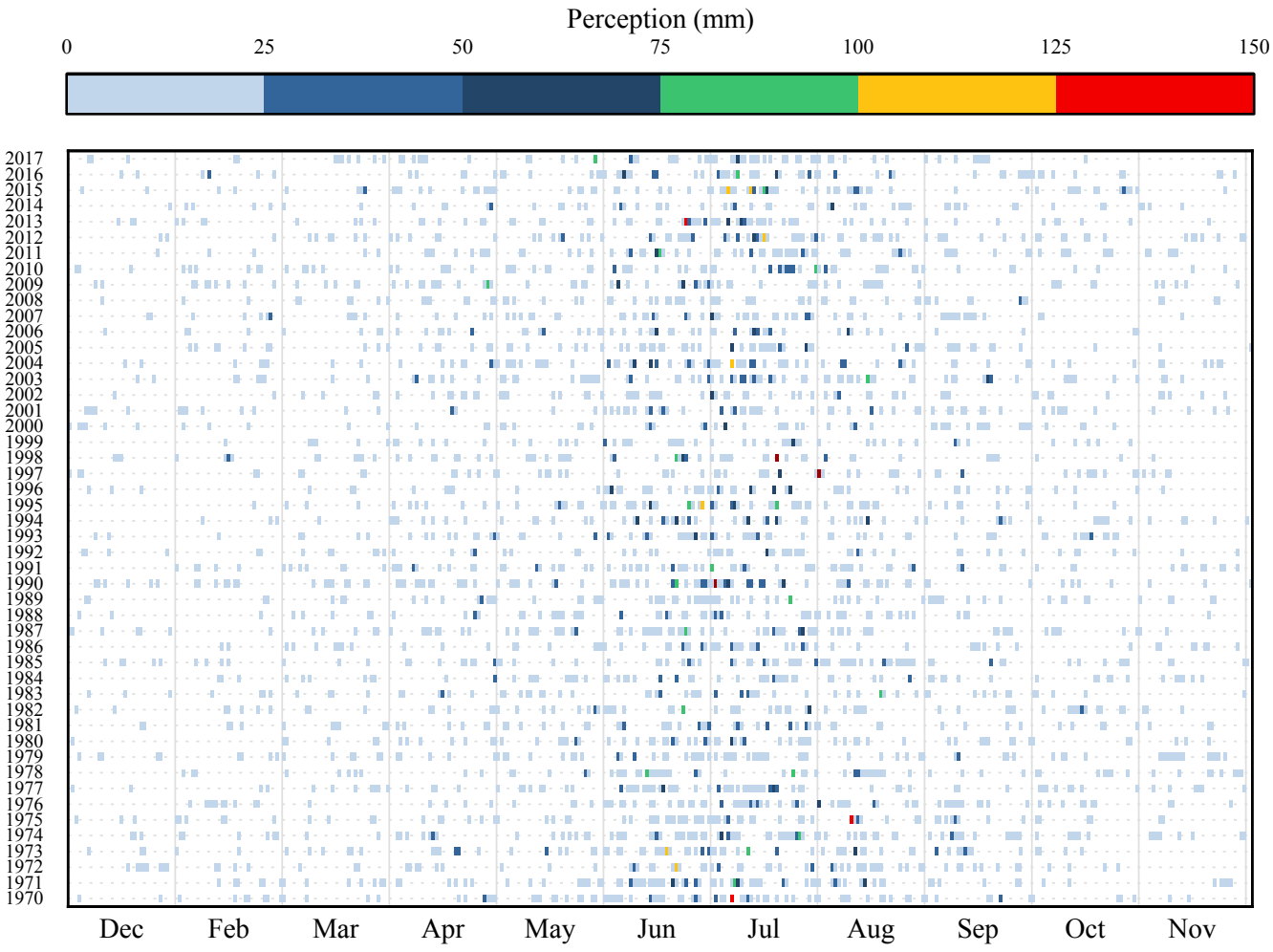

Fig. 6. Daily rainfall statistics in the study area from 1970 to 2017.

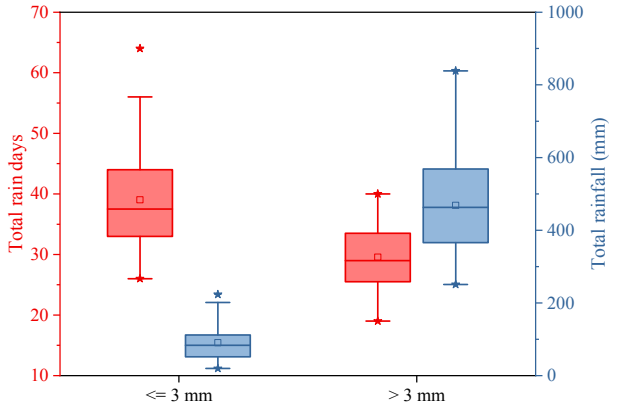

Fig. 7. Number of rainfall days and the corresponding total rainfall.

rainfall and amount of GHG emissions mitigated. The adjusted R^2 of the curve in Fig. 11 is 0.70, showing an obvious correlation between annual rainfall and rate of GHG emissions mitigated.

3.5. Curve fitting for the Pearson Type III distribution

After the construction of the SCDS in the study area, the total GHG emissions decreased by 3752.5 to 26238.9 tons with an average of 10677.3 tons–compared to a CSS–in the 48 hydrological scenarios used in this study. The Pearson Type III distribution curve was adopted to fit the benefit of the change in GHG emissions mitigation; the GHG emissions mitigation in different probabilities are shown in Fig. 12. Parameter selection and amount of GHG emissions mitigated correspond to a typical occurrence probability as shown in Table 4.

After the construction of a SCDS in the study area, total GHG emissions decreased by 25.9% to 68.7% with an average of 45.9%–compared to a CSS–in the 48 hydrological scenarios used in this study. The Pearson Type III distribution curve was adopted to plot the rate of change in the mitigation of GHG emissions. The GHG emissions mitigation at different occurrence probabilities are shown in Fig. 13. Parameter selection and the correspondence of the rate of mitigation of GHG emissions to typical occurrence probabilities are shown in Table 5.

As shown in Tables 4 and 5, the C_V values of the frequency analysis curves of the amount and rate of change are both small, indicating that the density of the two frequency distribution curves are less discrete and the frequency distribution is concentrated. The C_S values of the frequency analysis curves of both the amount and rate of change in GHG mitigation are both greater than 0; furthermore, the occurrence frequency corresponding to the mean value is less than 50% and thus indicates that both of the distribution curves are positively skewed distributions. This is consistent with the results that the rainfall levels in the study area are mainly low and medium, and the rainfall is positively correlated with GHG emissions mitigation benefits.

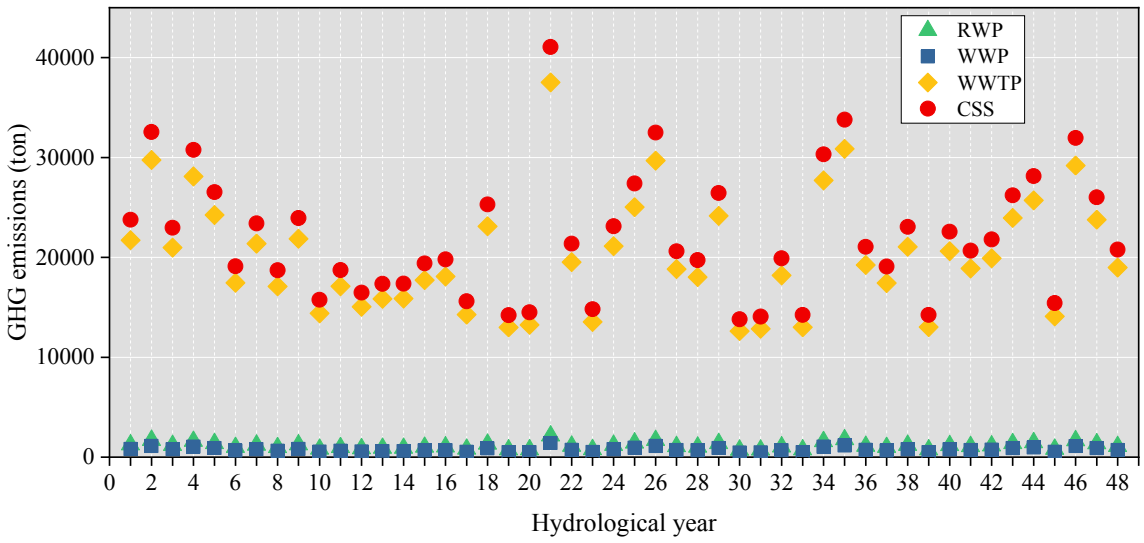

Fig. 8. GHG emissions levels from different attributable sources in CSS.

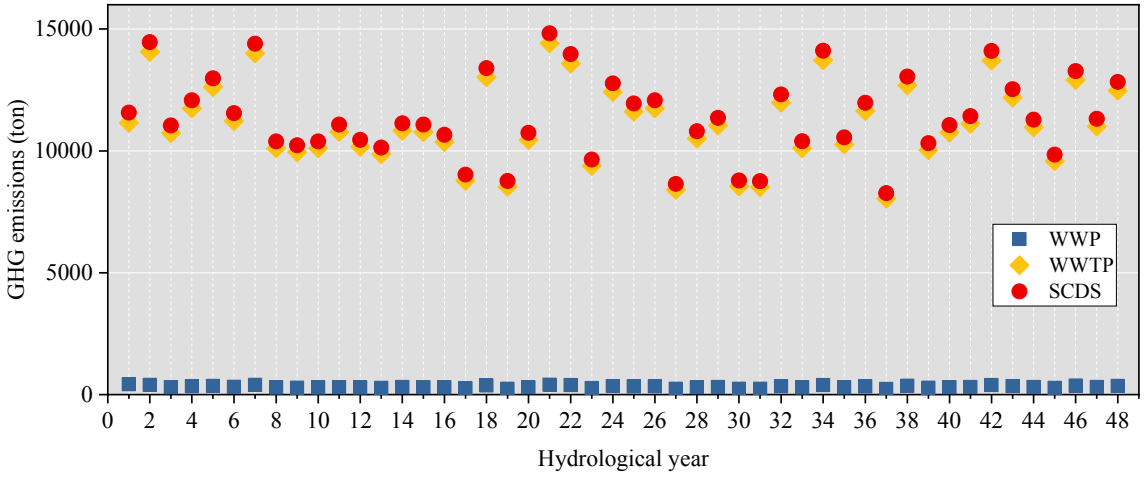

Fig. 9. GHG emissions levels from different attributable sources in SCDS.

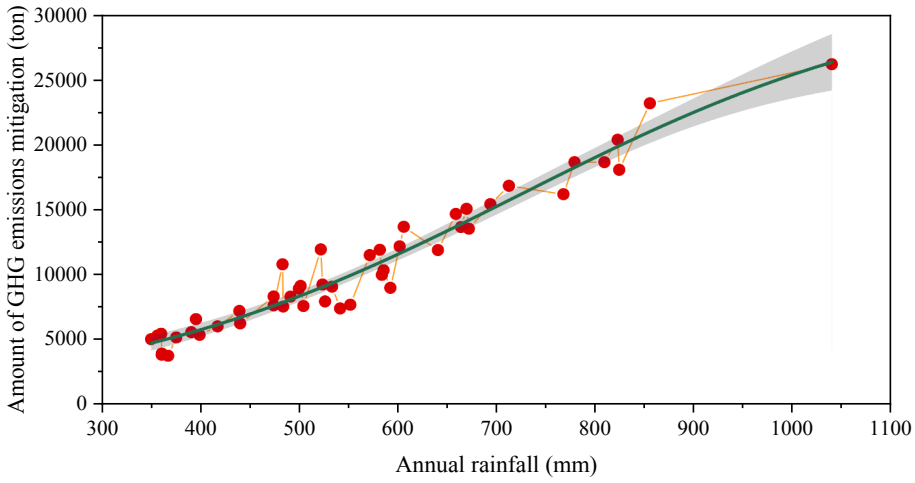

Fig. 10. Logistic curve (green) fitting the annual rainfall and amount of GHG emissions mitigated. The gray area is the 95% confidence interval.

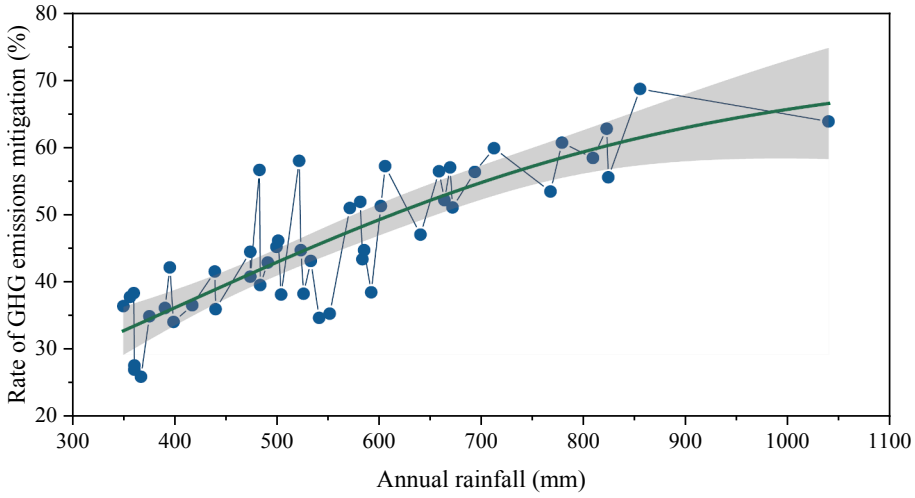

Fig. 11. Logistic curve (green) fitting the annual rainfall and rate of GHG emissions mitigated. The gray area is the 95% confidence interval.

Table 3
Parameter estimates and other statistics derived from the fit of the logistic function representing the relationship between rainfall and rates of GHG mitigation.

	Parameters			R^2
	a	b	k	
Annual rainfall and amount of GHG emissions mitigation	30324.13163.	30.41898.	0.00472.	0.95.
Annual rainfall and rate of GHG emissions mitigation	72.55342.	4.56477.	0.00378.	0.70.

3.6. Potential mitigation of GHG emissions via urban drainage systems

This study uses daily rainfall data from hydrological stations for the period 1970 to 2017 to calculate the benefits of using GI in mitigating GHG emissions. The application of GI in the hydrological cycle processes during rainfall events reduces the GHG emissions from WWPs, WWTPs, and RWPs. Over the 48 hydrological years examined, the average rate of GHG emissions mitigated was 45.9% and the average amount of GHG emissions mitigated annually was 10677.3 tons. There are many benefits to mitigating GHG emissions using GI in urban drainage. A non-linear fitting analysis based on a logistic curve showed, reasonably, that the amount and rate of GHG emissions mitigation increase with an increase in annual rainfall. The findings can provide a quantitative basis upon which local authorities can formulate goals and policies for energy conservation and GHG emissions reduction via GI-based urban drainage systems.

WWTPs are the main sources of GHG emissions in the urban drainage system [34] where, according to the results of this study, most of the

Table 4
Selected parameters and GHG emissions mitigated corresponding to a typical occurrence frequency.

Parameters				GHG emissions mitigated corresponding to a typical occurrence probability (P)/(ton)			
N	Mean (tons)	C_V	C_S/C_V	P = 20%	P = 50%	P = 75%	P = 95%
48	10677.29.	0.51.	2.57.	14592.2.	9527.9.	6653.5.	4160.3.

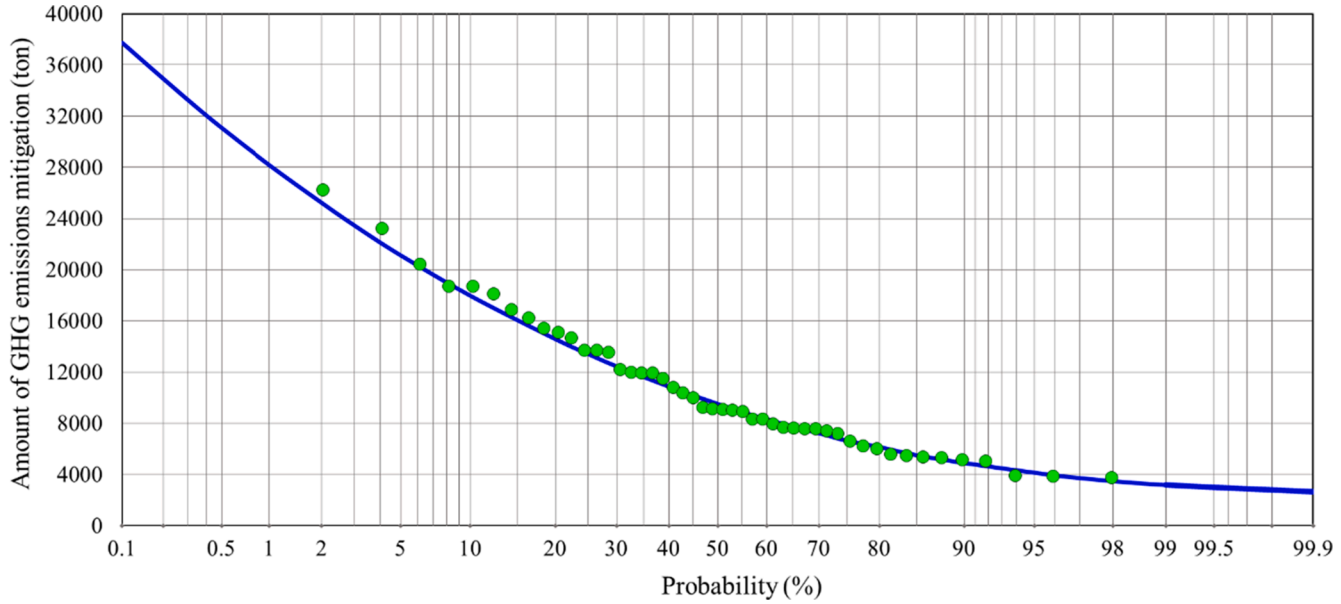

Fig. 12. Pearson Type III distribution curve for the amount of GHG emissions mitigated.

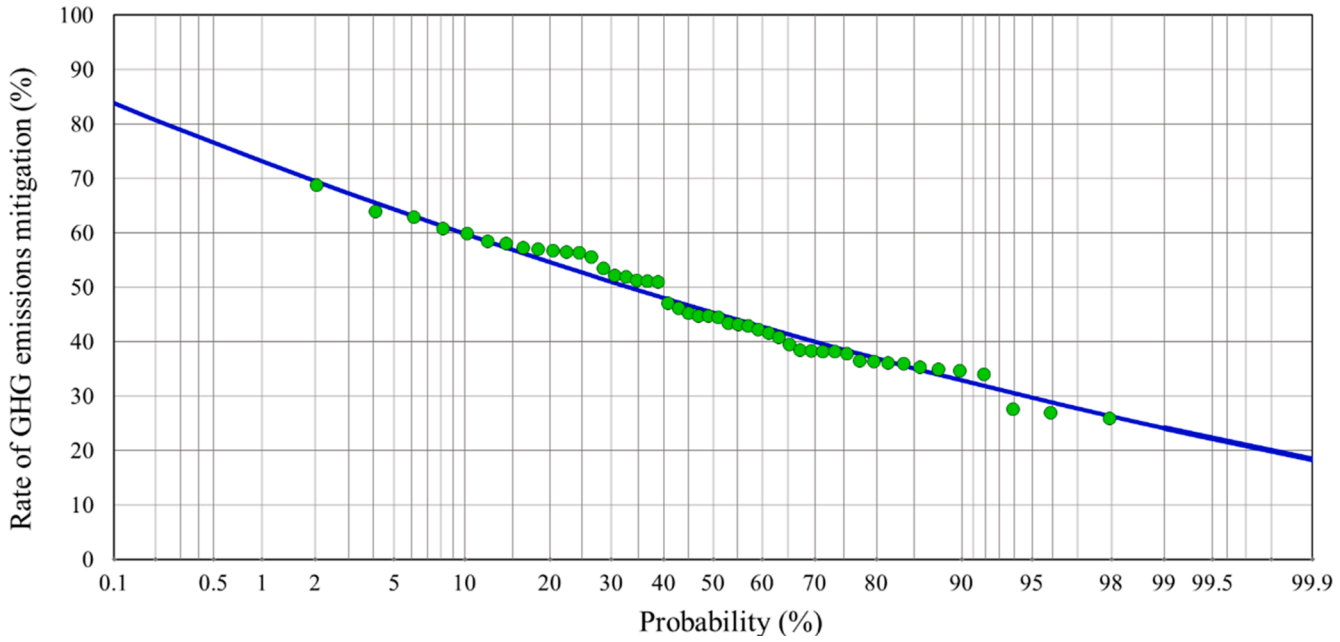

Fig. 13. Pearson Type III distribution curve for the rate at which GHG emissions are mitigated.

Table 5
Selected parameters and rate of GHG emissions mitigated corresponding to a typical occurrence frequency.

Parameters				Rate of GHG emissions mitigation corresponding to a typical occurrence probability (P)/(%)			
n	Mean (%)	C_V	C_S/C_V	P = 20%	P = 50%	P = 75%	P = 95%
48	45.92.	0.23.	1.5.	54.6.	45.3.	38.5.	29.7.

GHG emissions caused by rainwater runoff during rainfall events occur. The average GHG emissions from WWTPs–in a CSS–are 20181.1 tons and accounts for 91.4% of the total GHG emissions of the entire system. After the implementation of the SCDS, the initial rain runoff flows into WWTPs and rainwater runoff pollution is effectively controlled. During the runoff process, the WWTPs emit 11095.7 tons of GHGs that account for 97.2% of the total emissions from the entire SCDS. This still accounts for the vast majority of urban drainage systems which indicate that WWTPs are the main methods by which GHG emissions in the urban drainage system can be mitigated. To reduce these GHG emissions, the carbon neutralization of WWTPs has become an important topic of research around the world [50]. In China, achieving carbon neutrality will also become a top priority for WWTPs in the near future [51].

In terms of the pump system, this study focused on optimizing their

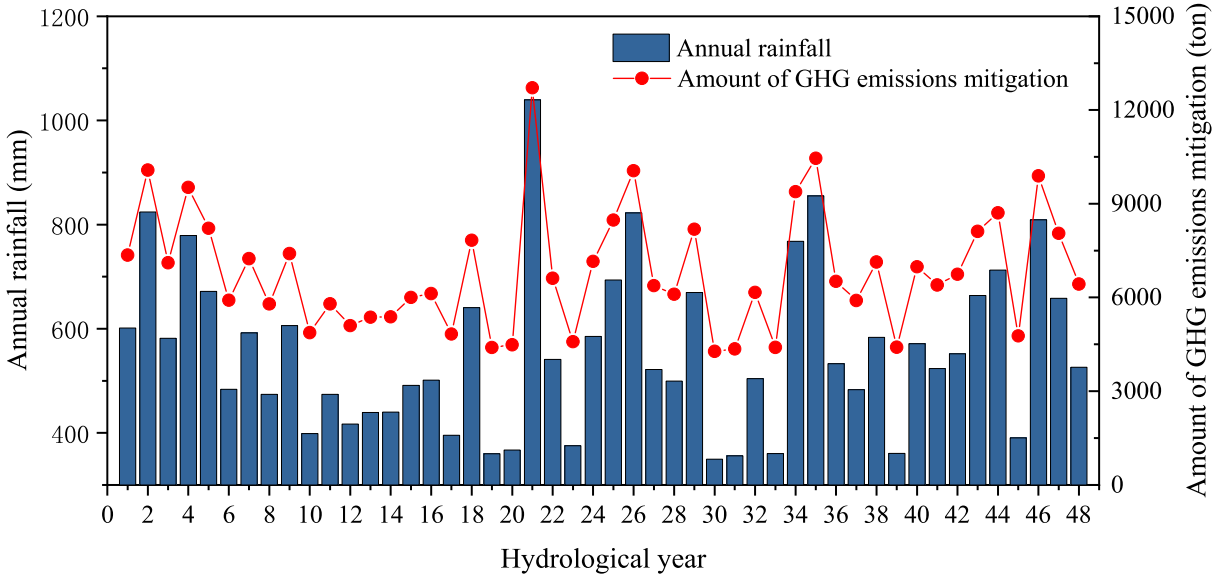

Fig. 14. Annual rainfall and the corresponding mitigation of GHG emissions in the water supply system.

energy utilization from the perspective of reducing pump load. Efficiency enhancement initiatives are considered another key solution in reducing overall energy consumption levels, particularly under conditions in which pump loads are uneven. Rational selection of pumps and the use of variable frequency drives [52] are ways in which the energy utilization efficiency of the pump system can be improved.

3.7. Reducing GHG emissions from water supply systems

Rapid urbanization and the expansion of metropolitan areas have resulted in severe demands on water and energy resources. Energy and water have become connected in nexus interactions such as the "water–energy nexus" [53]. GI indirectly reduces the GHG emissions of the urban water supply by recycling rainwater [54]. Presently, tap water is used for greening and maintaining the ecological environment in Dongying. After the implementation of the sponge city plan, rainwater can be stored and recovered through rainwater collection facilities that can effectively reduce a corresponding water supply. The return rate of rainwater could be 10% in a normal year. Therefore, if the consumption of tap water uses 0.65 kWh of power for its the treatment and supply [44], calculations based on a period of 48 hydrological years show that the GHG emissions from this system will be reduced by 4274.8 to 12709.3 tons, with an average of 6837.1 tons/a, in the study area. The annual amount of rainfall and the corresponding mitigation of GHG emissions from the water supply system are shown in Fig. 14.

3.8. Applications of this work

This study develops a framework that can be implemented in the assessment of GHG emissions mitigation from GI-based urban drainage systems. This, in turn, can be used to support policymaking and evaluation of urban-scale GHG emissions from urban drainage systems, especially for pioneering cities worldwide that actively implement GI practices. The results of the frequency distribution are a valuable reference by which to set the target standard for reducing GHG emissions in urban drainage systems. Furthermore, the practical case study of the SCDS in China has shown the considerable potential of the use of GIs to mitigate GHG emissions. Meanwhile, the assessment framework can be applied to a comprehensive assessment of the effectiveness of GI. In previous studies, assessments of energy efficiency were usually ignored, except in terms of the benefit of water quantity and quality. For policymakers or stakeholders making a decision between gray and green infrastructure alternatives, this study demonstrates the feasibility of implementation of the latter.

3.9. Limitations and directions for future research

GI also has certain additional effects on carbon reduction; these include mitigating the heat island effect [55], reducing the energy consumption of air conditioners [56], and sequestering carbon in vegetation [57]. In terms of the production of required raw materials, construction, and maintenance, GI consumes less energy than traditional drainage systems, over their entire life cycle [21]. This study only calculated the effect that optimizing rainwater runoff had on GHG reduction after the implementation of GI. Additional benefits of GHG mitigation, such as the mitigation of the heat island effect and sequestration of carbon in vegetation, were not quantified. Singh and Kansal [58] show that throughout its life, the energy consumed in the operation of a sewage discharge system accounts for a vast majority (70%) of the total energy consumed. This supports the validity of conclusion of this study. Kavehei et al. [28] evaluated the potential of different GIs to act as carbon sinks and found that the degree of the latter varies among different types of the former. Zölch et al. [59] pointed out that the potential of GI to reduce GHG emissions is not only related to the type and scale of the facilities but also to their planning and layout. Further comprehensive assessments of the potential of GI in mitigating GHG emissions would be an important direction for future research.

4. Conclusions

This study establishes a method by which the greenhouse gas emissions of the hydrological processes during rainfall events can be assessed at a city scale. This is done to assess the efficiency of GI to mitigate greenhouse gas emissions. The impact factor method is applied to analyze greenhouse gas emissions in the hydrological cycle of traditional and green infrastructure -based urban drainage systems. The amount and rate of change are adopted as assessments of the benefits of mitigating greenhouse gas emissions before and after implementation of green infrastructure. The results of a case study conducted in Dongying, China show that a green infrastructure -based urban drainage system has a substantial benefit in terms of mitigating greenhouse gas emissions. In this study, the annual greenhouse gas emissions of the urban drainage system were mitigated from 3752.5 to 26238.9 CO_2 equivalent tons, with an average of 10677.3 tons/a, after the implementation of green infrastructure. This corresponds to an improvement of 25.9–68.7% with an average of 45.9% compared to the results of a traditional urban drainage system. An analysis of the fit of the relationships between the amount and rate of change in the greenhouse gas emissions indicates that annual rainfall has a non-linear (positive) correlation for 48 hydrological scenarios tested. The effect of mitigating greenhouse gas emissions increases with the increase in rainfall in the green infrastructure -based urban drainage system. The probability of the occurrence of benefits from annual greenhouse gas emissions mitigation was analyzed for both factors using a Pearson Type III distribution curve; the result was a positively-skew distribution in both cases. This study has not considered additional benefits of greenhouse gas mitigation, such as the mitigation of the heat island effect and carbon sequestration in vegetation. More comprehensive assessments of the potential of green infrastructure to mitigate greenhouse gas emissions will be an important research theme in the future.

CRediT authorship contribution statement

Jiahong Liu: Conceptualization, Funding acquisition, Methodology, Writing - review & editing. **Jia Wang:** Data curation, Investigation, Methodology, Writing - original draft. **Xiangyi Ding:** Data curation, Investigation. **Weiwei Shao:** Data curation, Investigation. **Chao Mei:** Data curation, Investigation. **Zejin Li:** Writing - original draft. **Kaibo Wang:** Writing - original draft.

Declaration of Competing Interest

The authors declare that they have no known competing financial interests or personal relationships that could have appeared to influence the work reported in this paper.

Acknowledgments

This study was supported by the Chinese National Natural Science Foundation (No. 51739011 & No. 51979285), the National Key Research and Development Program of China (2016YFC0401401), and the Research Fund of the State Key Laboratory of Simulation and Regulation of Water Cycle in River Basin (No.2020ZY02).

References

[1] Nitschke CR, Nichols S, Allen K, Dobbs C, Livesley SJ, Baker PJ, et al. The influence of climate and drought on urban tree growth in southeast Australia and the implications for future growth under climate change. Landscape Urban Plann 2017;167:275–87. https://doi.org/10.1016/j.landurbplan.2017.06.012.

[2] Pesce M, Critto A, Torresan S, Giubilato E, Santini M, Zirino A, et al. Modelling climate change impacts on nutrients and primary production in coastal waters. Sci

Total Environ 2018;628:919–37. https://doi.org/10.1016/j.scitotenv.2018.02.131.
[3] WMO. Provisional WMO Statement on the Status of the Global Climate in 2018; 2018. <https://environmentalmigration.iom.int/wmo-provisional-statement-state-global-climate-2018> [accessed on 28/12/2019].
[4] Roberts SH, Foran BD, Axon CJ, Warr BS, Goddard NH. Consequences of selecting technology pathways on cumulative carbon dioxide emissions for the United Kingdom. Appl Energy 2018;228:409–25. https://doi.org/10.1016/j.apenergy.2018.06.078.
[5] Herran DS, Tachiiri K, Matsumoto K. Global energy system transformations in mitigation scenarios considering climate uncertainties. Appl Energy 2019;243:119–31. https://doi.org/10.1016/j.apenergy.2019.03.069.
[6] Tan S, Yang J, Yan J, Lee C, Hashim H, Chen B. A holistic low carbon city indicator framework for sustainable development. Appl Energy 2017;185:1919–30. https://doi.org/10.1016/j.apenergy.2016.03.041.
[7] Shao L, Li Y, Feng K, Meng J, Shan Y, Guan D. Carbon emission imbalances and the structural paths of Chinese regions. Appl Energy 2018;215:396–404. https://doi.org/10.1016/j.apenergy.2018.01.090.
[8] Liu X, Duan Z, Shan Y, Duan H, Wang S, Song J. Low-carbon developments in Northeast China: Evidence from cities. Appl Energy 2019;236:1019–33. https://doi.org/10.1016/j.apenergy.2018.12.060.
[9] Martin C, Kamara O, Berzosa I, Badiola JL. Smart GIS platform that facilitates the digitalization of the integrated urban drainage system. Environ Modell Software 2020;123:104568. https://doi.org/10.1016/j.envsoft.2019.104568.
[10] Mikosz J. Analysis of greenhouse gas emissions and the energy balance in a model municipal wastewater treatment plant. Desalin Water Treat 2016;57(59):28551–9. https://doi.org/10.1080/19443994.2016.1192491.
[11] Li C, Liu M, Hu Y, Hu Y, Shi T, Qu X, et al. Effects of urbanization on direct runoff characteristics in urban functional zones. Sci Total Environ 2018;643:301–11. https://doi.org/10.1016/j.scitotenv.2018.06.211.
[12] Kumar P, Masago Y, Mishra BK, Fukushi K. Evaluating future stress due to combined effect of climate change and rapid urbanization for Pasig-Marikina River, Manila. Groundwater for Sustain Devel 2018;6:227–34. https://doi.org/10.1016/j.gsd.2018.01.004.
[13] Casal-Campos A, Sadr SMK, Fu G, Butler D. Reliable, resilient and sustainable urban drainage systems: an analysis of robustness under deep uncertainty. Environ Sci Technol 2018;52(16):9008–21. https://doi.org/10.1021/acs.est.8b01193.
[14] Dong X, Guo H, Zeng S. Enhancing future resilience in urban drainage system: Green versus grey infrastructure. Water Res 2017;124:280–9. https://doi.org/10.1016/j.watres.2017.07.038.
[15] Thacker S, Adshead D, Fay M, Csordas S. Infrastructure for sustainable development. Nat Sustainability 2019;2(4):324. https://doi.org/10.1596/978-0-8213-8518-0.
[16] Launay MA, Dittmer U, Steinmetz H. Organic micropollutants discharged by combined sewer overflows–Characterisation of pollutant sources and rainwater-related processes. Water Res 2016;104:82–92. https://doi.org/10.1016/j.watres.2016.07.068.
[17] Xu C, Jia M, Xu M, Long Y, Jia H. Progress on environmental and economic evaluation of low-impact development type of best management practices through a life cycle perspective. J. Clean. Prod. 2019;213:1103–14.
[18] Mei C, Liu J, Wang H, Yang Z, Ding X, Shao W. Integrated assessments of green infrastructure for flood mitigation to support robust decision-making for sponge city construction in an urbanized watershed. Sci Total Environ 2018;639:1394–407. https://doi.org/10.1016/j.scitotenv.2018.05.199.
[19] Fletcher TD, Shuster W, Hunt WF, Ashley R, Butler D, Arthur S, et al. SUDS, LID, BMPs, WSUD and more–The evolution and application of terminology surrounding urban drainage. Urban Water J 2015;12(7):525–42. https://doi.org/10.1080/1573062X.2014.916314.
[20] Li C, Peng C, Chiang P, Cai Y, Wang X, Yang Z. Mechanisms and applications of green infrastructure practices for rainwater control: A review. J Hydrol 2018;568:626–37. https://doi.org/10.1016/j.jhydrol.2018.10.074.
[21] Casal-Campos A, Fu G, Butler D. The whole life carbon footprint of green infrastructure: A call for integration. NOVATECH 2013. 2013.
[22] Rodríguez-Sinobas L, Zubelzu S, Perales-Momparler S, Canogar S. Techniques and criteria for sustainable urban rainwater management. The case study of Valdebebas (Madrid, Spain). J Cleaner Prod 2018;172:402–16. https://doi.org/10.1016/j.jclepro.2017.10.070.
[23] Matthews T, Lo AY, Byrne JA. Reconceptualizing green infrastructure for climate change adaptation: Barriers to adoption and drivers for uptake by spatial planners. Landscape Urban Plann 2015;138:155–63. https://doi.org/10.1016/j.landurbplan.2015.02.010.
[24] De Sousa MR, Montalto FA, Spatari S. Using life cycle assessment to evaluate green and grey combined sewer overflow control strategies. J Ind Ecol 2012;16(6):901–13. https://doi.org/10.1111/j.1530-9290.2012.00534.x.
[25] Wang R, Eckelman MJ, Zimmerman JB. Consequential environmental and economic life cycle assessment of green and gray rainwater infrastructures for combined sewer systems. Environ Sci Technol 2013;47(19):11189–98. https://doi.org/10.1021/es4026547.
[26] Moore TLC, Hunt WF. Predicting the carbon footprint of urban rainwater infrastructure. Ecol Eng 2013;58:44–51. https://doi.org/10.1016/j.ecoleng.2013.06.021.
[27] Bouchard NR, Osmond DL, Winston RJ, Hunt WF. The capacity of roadside vegetated filter strips and swales to sequester carbon. Ecol Eng 2013;54:227–32. https://doi.org/10.1016/j.ecoleng.2013.01.018.
[28] Kavehei E, Jenkins GA, Adame MF, Lemckert C. Carbon sequestration potential for mitigating the carbon footprint of green rainwater infrastructure. Renew Sustain Energy Rev 2018;94:1179–91. https://doi.org/10.1016/j.rser.2018.07.002.
[29] Bevilacqua P, Mazzeo D, Bruno R, Arcuri N. Surface temperature analysis of an extensive green roof for the mitigation of urban heat island in southern mediterranean climate. Energy Build 2017;150:318–27. https://doi.org/10.1016/j.enbuild.2017.05.081.
[30] He Y, Yu H, Dong N, Ye H. Thermal and energy performance assessment of extensive green roof in summer: A case study of a lightweight building in Shanghai. Energy Build 2016;127:762–73. https://doi.org/10.1016/j.enbuild.2016.06.016.
[31] Berardi U, GhaffarianHoseini AH, GhaffarianHoseini A. State-of-the-art analysis of the environmental benefits of green roofs. Appl Energy 2014;115:411–28. https://doi.org/10.1016/j.apenergy.2013.10.047.
[32] Devkota J, Schlachter H, Apul D. Life cycle based evaluation of harvested rainwater use in toilets and for irrigation. J Cleaner Prod 2015;95:311–21. https://doi.org/10.1016/j.jclepro.2015.02.021.
[33] Cai B, Cui C, Zhang D, Cao L, Wu P, Pang L, et al. China city-level greenhouse gas emissions inventory in 2015 and uncertainty analysis. Appl Energy 2019;253:113579. https://doi.org/10.1016/j.apenergy.2019.113579.
[34] Mannina G, Butler D, Benedetti L, Deletic A, Fowdar H, Fu G, et al. Greenhouse gas emissions from integrated urban drainage systems: Where do we stand? J Hydrol 2018;559:307–14. https://doi.org/10.1016/j.jhydrol.2018.02.058.
[35] Eaton TT. Approach and case-study of green infrastructure screening analysis for urban rainwater control. J Environ Manage 2018;209:495–504. https://doi.org/10.1016/j.jenvman.2017.12.068.
[36] Chen J, Liu Y, Gitau MW, Engel BA, Flanagan DC, Harbor JM. Evaluation of the effectiveness of green infrastructure on hydrology and water quality in a combined sewer overflow community. Sci Total Environ 2019;665:69–79. https://doi.org/10.1016/j.scitotenv.2019.01.416.
[37] Birtchnell T, Gill N, Sultana R. Sleeper cells for urban green infrastructure: Harnessing latent competence in greening Dhaka's slums. Urban For Urban Green 2019;40:93–104. https://doi.org/10.1016/j.ufug.2018.05.014.
[38] Yan X, Qiu D, Guo D, Qi X, Zheng S, Cheng K, Liu J. Emission Inventory of Greenhouse Gas from Urban Wastewater Treatment Plants and Its Temporal and Spatial Distribution in China. Huan jing ke xue= Huanjing kexue 2018;39(3):1256–63. https://doi.org/10.13227/j.hjkx.201706079 [in Chinese].
[39] Kosse P, Lübken M, Schmidt TC, Lange RL, Wichern M. Assessing potential impacts of phosphate precipitation on nitrous oxide emissions and the carbon footprint of wastewater treatment plants. Environ Technol 2019;40(16):2107–13. https://doi.org/10.1080/09593330.2018.1437781.
[40] Wu X, Xia X, Chen G, Wu X, Chen B. Embodied energy analysis for coal-based power generation system-highlighting the role of indirect energy cost. Appl Energy 2016;184:936–50. https://doi.org/10.1016/j.apenergy.2016.03.027.
[41] Yan X, Li L, Liu J. Characteristics of greenhouse gas emission in three full-scale wastewater treatment processes. J Environ Sci 2014;26(2):256–63. https://doi.org/10.1016/S1001-0742(13)60429-5.
[42] Daelman MR, van Voorthuizen EM, van Dongen UG, Volcke EI, van Loosdrecht MC. Seasonal and diurnal variability of N2O emissions from a full-scale municipal wastewater treatment plant. Sci Total Environ 2015;536:1–11. https://doi.org/10.1016/j.scitotenv.2015.06.122.
[43] Department of climate change, national development and reform commission. Baseline emission factor of China's regional power grid in 2017, 2018 [in Chinese].
[44] Liu J, Wang D, Xiang C, et al. Assessment of the Energy Use for Water Supply in Beijing. Energy Procedia 2018;152:271–80. https://doi.org/10.1016/j.egypro.2018.09.122.
[45] Guo F, Wu Y, Li B, Li Z, Zhou P, Wu G. Research status and development trend for energy saving in municipal wastewater treatment plants in China. Technol Water Treatm 2017(06):7–10+16 [in Chinese].
[46] IPCC. Climate change (2013). The physical science basis. In Contribution of Working Group I to the Fifth Assessment Report of the Intergovernmental Panel on Climate Change. Cambridge, United Kingdom and New York, NY, USA: Cambridge University Press; 2013, p. 1535.
[47] Chen L, Tao Z, Kai P, et al. Study on carbon emission of sponge city rainwater system based on life cycle assessment. Environ Sustain Devel 2019(1):132–7 [in Chinese].
[48] Demir Ö, Yapıcıoğlu P. Investigation of GHG emission sources and reducing GHG emissions in a municipal wastewater treatment plant. Greenhouse Gases Sci Technol 2019;9(5):948–64. https://doi.org/10.1002/ghg.1912.
[49] Zhou T, Roorda MJ, MacLean HL, Luk J. Life cycle GHG emissions and lifetime costs of medium-duty diesel and battery electric trucks in Toronto, Canada. Transp Res Part D: Transp Environ 2017;55:91–8. https://doi.org/10.1016/j.trd.2017.06.019.
[50] Zhao X, Jin X, Guo W, Zhang C, Shan Y, Du M. China's urban methane emissions from municipal wastewater treatment plant. Earth's Future 2019;7(4):480–90. https://doi.org/10.1029/2018EF001113.
[51] Hao X, Liu R, Huang X. Evaluation of the potential for operating carbon neutral WWTPs in China. Water Res 2015;87:424–31. https://doi.org/10.1016/j.watres.2015.05.050.
[52] Shankar VKA, Umashankar S, Paramasivam S, Hanigovszki N. A comprehensive review on energy efficiency enhancement initiatives in centrifugal pumping system. Appl Energy 2016;181:495–513. https://doi.org/10.1016/j.apenergy.2016.08.070.
[53] Fang D, Chen B. Linkage analysis for the water–energy nexus of city. Appl Energy 2017;189:770–9. https://doi.org/10.1016/j.apenergy.2016.04.020.

[54] Liu L, Jensen MB. Green infrastructure for sustainable urban water management: Practices of five forerunner cities. Cities 2018;74:126–33. https://doi.org/10.1016/j.cities.2017.11.013.
[55] Herath H, Halwatura RU, Jayasinghe GY. Evaluation of green infrastructure effects on tropical Sri Lankan urban context as an urban heat island adaptation strategy. Urban For Urban Greening 2018;29:212–22. https://doi.org/10.1016/j.ufug.2017.11.013.
[56] Strohbach MW, Arnold E, Haase D. The carbon footprint of urban green space—A life cycle approach. Landscape Urban Plann 2012;104(2):220–9. https://doi.org/10.1016/j.landurbplan.2011.10.013.
[57] Jim CY. Air-conditioning energy consumption due to green roofs with different building thermal insulation. Appl Energy 2014;128:49–59. https://doi.org/10.1016/j.apenergy.2014.04.055.
[58] Singh P, Kansal A. Energy and GHG accounting for wastewater infrastructure. Resour Conserv Recycl 2018;128:499–507. https://doi.org/10.1016/j.resconrec.2016.07.014.
[59] Zölch T, Maderspacher J, Wamsler C, Pauleit S. Using green infrastructure for urban climate-proofing: An evaluation of heat mitigation measures at the micro-scale. Urban For Urban Greening 2016;20:305–16. https://doi.org/10.1016/j.ufug.2016.09.011.